Finite Amplitude Disturbances Interaction with Premixed Laminar Flames

Mohamad Aslani, Jonathan D. Regele
Department of Aerospace Engineering, Iowa State University
Ames, IA, USA

1 Introduction

Combustion devices suffer from a wide range of disturbances. For instance, in land based gas turbines, flame blowoff and flashback due to pressure oscillations can result from the coupling of an acoustic field with induced unsteady heat release [1]. Also, compression waves are created in internal combustion (IC) engines by rapid auto-ignition in localized hot spots of the fuel and air mixture. These waves interact with the burning medium and may cause engine knock or even fatal damage. Understanding the roles played by these interactions are important in designing efficient engines. Especially, because these events are most likely to happen when the engines are designed to operate near their combustion limits. [2].

Previous studies in this area are mostly focused on either acoustic or strong shock wave interaction, with less information about the wide spectrum of behaviors that may exist between these two extremes. For example the interaction of a flame and a finite amplitude disturbance is not well characterized. Studies on the interaction of a flame with a shock wave goes back to Markstein's early experiments [3]. Khokhlov *et al.* performed a series of 2-D and 3-D numerical simulations to understand this interaction in the context of deflagration to detonation transition [4]. A more recent study addressed the interaction of an expansion wave (a slow/fast medium as opposed to fast/slow made by a shock wave) with a laminar premixed flame [5].

In this work, we study the interaction of a finite amplitude disturbance with a laminar premixed flame. To quantify the interaction, a compression wave is characterized based upon appropriate length scales, in this case, the laminar flame thickness. By looking at the early interaction time, we study the flame geometry, increase in fuel consumption rate and burning speed for a range of short to long compression waves.

2 Problem statement and numerical modeling

To simulate a finite amplitude compression wave interaction with a laminar premixed flame, we solve the 2-D reactive Navier-Stokes (N-S) equations coupled with Fick's law for transport and diffusion:

Correspondence to: jregele@iastate.edu

$$\begin{aligned}
\frac{\partial \rho}{\partial t} + \nabla \cdot (\rho \mathbf{U}) &= 0 \\
\frac{\partial (\rho \mathbf{U})}{\partial t} + \nabla \cdot (\rho \mathbf{U}\mathbf{U}) + \nabla \cdot \hat{\sigma} &= 0 \\
\frac{\partial (\rho E)}{\partial t} + \nabla \cdot (\rho \mathbf{U} E) + \nabla \cdot (\mathbf{U} \cdot \hat{\sigma}) + \nabla \cdot (k \nabla T) &= q\dot{\omega} \\
\frac{\partial (\rho Y_f)}{\partial t} + \nabla \cdot (\rho \mathbf{U} Y_f) + \nabla \cdot (\rho D \nabla Y_f) &= -\dot{\omega},
\end{aligned} \tag{1}$$

where $\rho, \mathbf{U}, E$ and T are density, velocity, total non-chemical energy and temperature, respectively. The tensor $\hat{\sigma}$ is defined as $-p\hat{I} + \hat{\tau}$, in which p is the static pressure ($\hat{I}$ is the identity matrix) and $\hat{\tau}$ is the viscous stress tensor for the compressible N-S equations. Transport parameters k and D are the thermal conduction and mass diffusion coefficients. Here, q is the chemical heat release per unit mass of fuel and $\dot{\omega}$ is the reaction rate defined by one-step Arrhenius chemical kinetics, i.e $\dot{\omega} = A\rho Y_f \exp(-\frac{T_a}{T})$. The activation temperature and pre-exponential factor are denoted by T_a and A. The parameters of the system were selected to produce the same laminar flame velocity ($S_f \sim 0.25\ m/s$), flame thickness ($l_f \sim 9 \times 10^{-5}\ m$) and adiabatic flame temperature ($T_{ad} = 2340\ K$) for a stoichiometric methane-air mixture at atmospheric pressure [6]. To close the system of non-linear equations, we used the ideal gas equation of state ($p = \rho RT$).

The non-dimensional form of these equations obtained by using ρ_0 (density of air at $T_0 = 300K$), c_0 (speed of sound: $\sqrt{\gamma RT_0}$) and l_f which lead to the following non-dimensional numbers:

$$Re = \frac{c_0 l_f}{\nu}, \quad Le = \frac{k}{\rho C_p D}, \quad Sc = \frac{\nu}{D}, \quad Pr = \frac{Sc}{Le}. \tag{2}$$

For the purpose of simplicity, in this study, we set $Le = Sc = 1$ which provides equal rates of diffusion and heat conduction.

2-D simulations of a compression wave impacting a perturbed laminar premixed flame interface are performed. The model compression wave is composed of a shock wave followed by a centered expansion wave. Then, the initial distribution across the expansion fan is the isentropic wave relation for the density, velocity and pressure. The compression wave is characterized by the pressure ratio or Mach number (M) of the shock and a compression wavelength ratio α. This wavelength is expressed as the ratio of the length of the expansion fan to the flame thickness: $\alpha = \lambda / l_f$. Therefore, a small value for α will model a weak compression wave and increasing it will strengthen the compression wave. If α is set to infinity then the compression wave will be a shock wave. In this paper, our results are based on a $1.67(3.0)$ Mach number (pressure ratio) shock wave and for four values of $\alpha = (0.1, 1.0, 10.0, \infty)$. This range is selected to provide a general understanding of this interaction. Figure 1 (a) shows a schematic of our 2-D domain. The flame interface is perturbed by a given sinusoidal perturbation amplitude ($a = 0.4 l_f$) and wavelength (which in our case is the channel height: $h_c = 2 l_f$). Therefore the flame surface is perturbed by $x_p = a \cos(2\pi y / h_c)$. Figure 1 (b) illustrates the position of the compression wave and the flame by plotting the distribution of the density across the center line of the domain.

The governing equations are solved using the parallel adaptive wavelet collocation method (PAWCM) [7]. The PAWCM platform uses wavelet thresholding to dynamically minimize the necessary grid points to the desired level of accuracy (See red dots on Figure 1 (b)). Crank-Nicolson time integration with a central spatial discretization is used. A hyperbolic solver [8] is used along with this method that carefully incorporates localized numerical dissipation terms. In this way spatial discretization maintains second order accuracy in smooth regions. In order to maintain the desired accuracy of the simulations, at least 70 points are used to resolve the flame. This level of accuracy is sufficient to study the evolution of the flame.

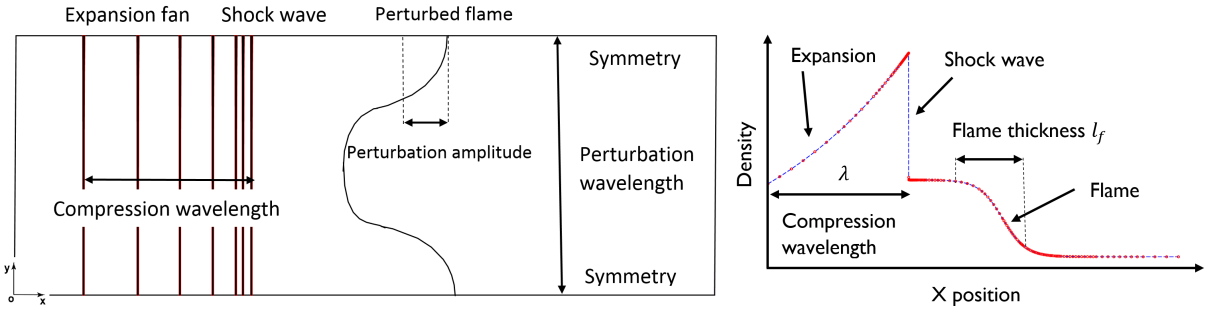

(a) 2D computational domain (b) Density distribution along the center line

Figure 1: Initial condition and density distribution

3 Results

Figures 2 and 3 show the details of the interaction by looking at density contours for the four different α values at six different acoustic times ($t_a = tl_f/c_0$) which correspond to the initial condition, incident shock, flame folding and evolution in the channel: $t_a = 0,\ 0.75,\ 2.5,\ 5.0,\ 8.5,\ 12.5$. According to these figures, all of the cases form a funnel of unburned materials that penetrates into the burned hot products. The length of the funnels are dependent on the characteristics of the initial incident compression wave. For the shortest compression wave ($\alpha = 0.1$, Figure2 (a)), in which the wavelength is an order of magnitude smaller than the flame thickness, a small funnel is formed. The length of the funnel increases for moderate ($\alpha = 1.0$, Figure2 (b)) and long ($\alpha = 10.0$, Figure3 (a)) compression waves; a longer funnel is seen in these cases because the flame has experienced a longer wave or period of density and momentum gradients.

As discussed in the previous section, an infinite length compression wave ($\alpha = \infty$) resembles a shock wave. The problem of shock wave interaction with a perturbed density interface has been studied thoroughly in the literature with the context of Richtmyer-Meshkov instability. Figure3 (b) shows this interaction. Similar behavior is observed in this case compared to the moderate and long compression wave, especially, in the first three snapshots. However, in the shock case the reaction rate increases steadily because the heated unburned gases (higher density) are being fed into the funnel and burn rapidly.

After these early times the flame shapes become significantly different. The edges of the shock wave case role into itself without any more stretching in the center section. However, for the moderate and long compression wave cases, the top head of the flame moves faster in the lighter fluid compared to the edges of the flame. This causes the flame to stretch more compared to the shock case where the whole flame area is advected by the post shock velocity.

The finite amplitude compression waves altered the physics of the flame in two ways: increasing the reactant's density and temperature and stretching the flame. To isolate these effects, it is useful to calculate and study the evolution of the flame surface area, fuel consumption rate and burning speed.

To find the flame surface area in these 2-D simulations, the length of iso-contour curves of fuel mass fraction $Y_f = 0.5$ were calculated. This method finds an accurate estimation of the flame length, although it may have errors when the flame folds into itself or a pocket is separated from the flame structure and burns. The global fuel consumption rate is simply calculated by a surface integral of the fuel reaction rate, $\dot{\Omega}_f = \int \dot{\omega}_f dA$.

Figure 4(a) shows the flame surface area as a function of acoustic time t_a for the four cases. All cases show identical behavior prior to the disturbance incident ($t_a < 2.0$). As the flame evolves, the flame surface areas differentiate. A smaller rate of increase for the short compression wave with $\alpha = 0.1$

is observed compared to other cases. The rate of increase for a compression wave of moderate size ($\alpha = 1.0 \sim 10$) is higher compared to a shock wave. For instance, at $t_a = 8.0$, the flame surface area of a compression wave is twice the shock wave case. The sudden drop in $\alpha = 10.0$ case at about $t_a = 10.0$ corresponds to the moment when a pocket is separated from the flame structure and burned relatively quickly after the separation.

The global fuel consumption rate of Figure 4(b), shows that a longer compression wave creates a higher rate of increase in the energy release rate. This rate is two times bigger for a shock wave compared to the longest compression wave because of the continued addition of fresh heated reactants into the flame. This rate is smaller for compression waves and decreases as α decreases.

It is also useful to look at the average burning speed: $S = \dot{\Omega}_f / A_f$. As it can be see from Figure 4(c), the burning speed is nearly equal for all cases at the beginning ($t_a < 1.5$). This rate, however, converges to a quasi-steady magnitude for the compression waves and increases linearly for a shock wave ($t_a > 2.5$). Therefore, it can be inferred that a significant portion of increase in fuel consumption rate for the compression waves is due to the increase in flame surface area and not the reaction mechanism. This is in contrast with the shock wave case in which an almost constant linear increase in burning speed is observed.

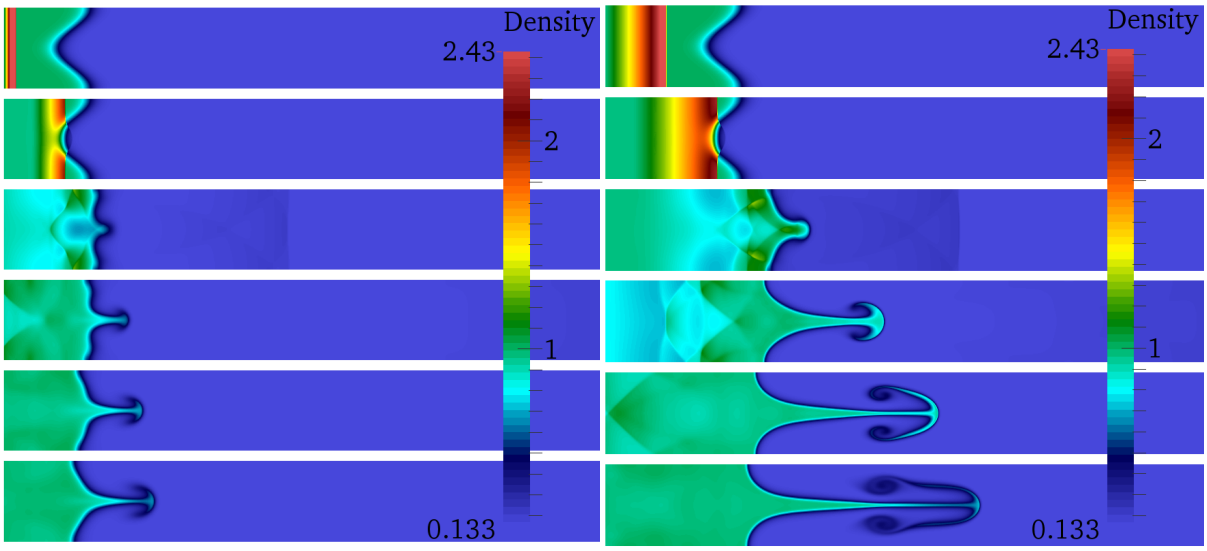

(a) $\alpha = 0.1$ (b) $\alpha = 1.0$

Figure 2: Density contours for short and moderate compression waves.

Conclusion

We study the interaction of finite amplitude compression waves with a premixed laminar flame using a 2-D simulation. The compression wave is idealized by a shock wave followed by a centered expansion wave. A rapid increase in reaction rate and flame surface area is observed in all cases during the early interaction of the compression wave and flame. However, after this interaction the fuel consumption rate and flame surface area varies as a function of disturbance wave length λ and flame thickness l_f.

For a short length disturbance i.e. $\lambda/l_f = 0.1$, the growth in flame surface area and reaction rate is lower than moderate and long disturbances ($\lambda/l_f = 1.0 \sim 10.0$). Since the flame is advected with the

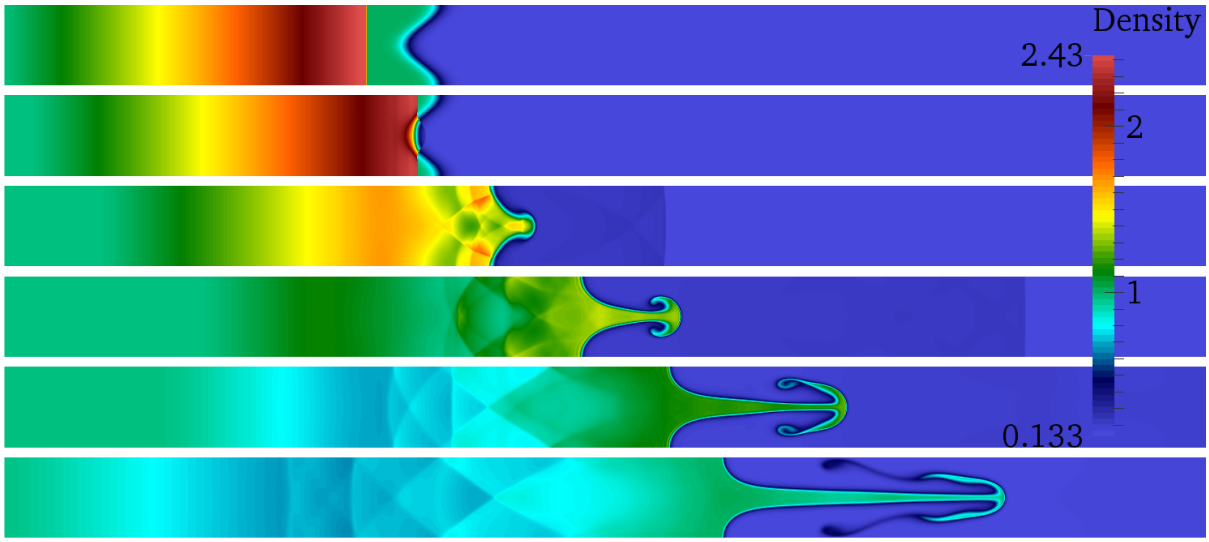

(a) $\alpha = 10.0$

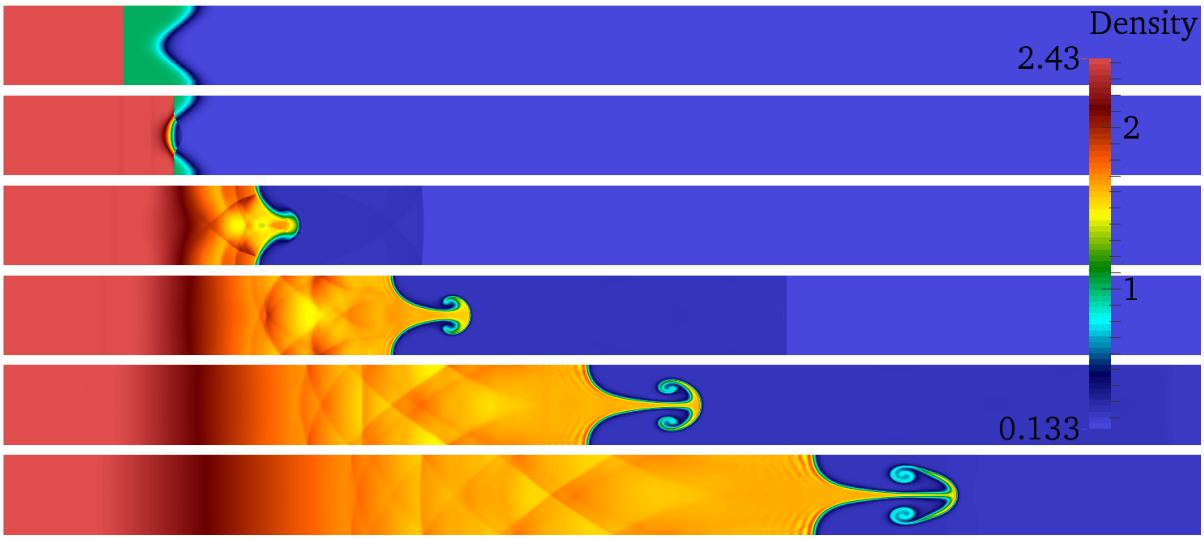

(b) $\alpha = \infty$

Figure 3: Density contours for a long compression wave and a shock wave.

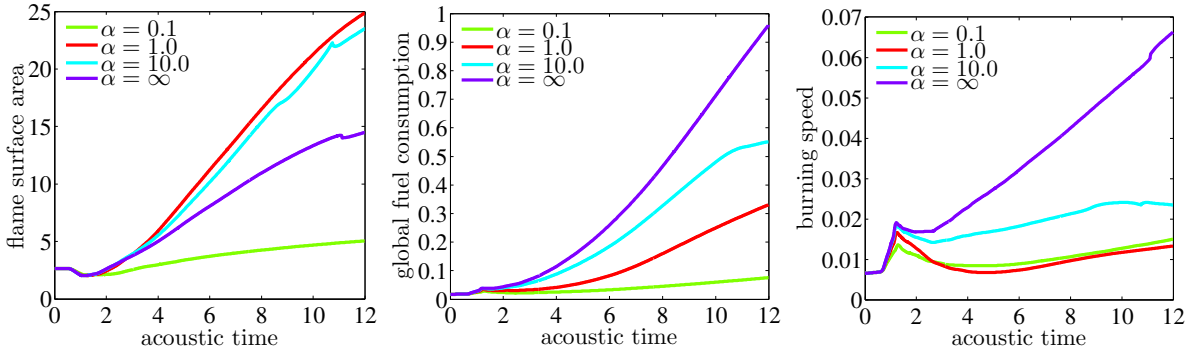

(a) Evolution of flame surface area (b) Global fuel consumption rate (c) Burning speed

Figure 4: Flame surface are, fuel consumption and burning speed versus acoustic time

post-shock velocity in the shock induced case ($\lambda/l_f = \infty$), the flame surface area growth for a shock wave grows at roughly half the rate as the moderate and long cases. Finally, the burning velocity is quasi-steady for finite amplitude compression waves and a linear growth rate is observed for a shock induced case.

References

[1] T. C. Lieuwen and V. Yang, "Combustion instabilities in gas turbine engines(operational experience, fundamental mechanisms and modeling)," *Progress in astronautics and aeronautics*, 2005.

[2] C. Dahnz, K.-M. Han, U. Spicher, M. Magar, R. Schiessl, and U. Maas, "Investigations on pre-ignition in highly supercharged SI engines," SAE Technical Paper, Tech. Rep., 2010.

[3] G. Markstein, "A shock-tube study of flame front-pressure wave interaction," in *Symposium (International) on Combustion*, vol. 6, no. 1. Elsevier, 1957, pp. 387–398.

[4] A. Khokhlov, E. Oran, and G. Thomas, "Numerical simulation of deflagration-to-detonation transition: the role of shock–flame interactions in turbulent flames," *Combustion and Flame*, vol. 117, no. 1, pp. 323–339, 1999.

[5] V. Kilchyk, R. Nalim, and C. Merkle, "Laminar premixed flame fuel consumption rate modulation by shocks and expansion waves," *Combustion and Flame*, vol. 158, no. 6, pp. 1140–1148, 2011.

[6] T. Poinsot, D. Veynante *et al.*, "Theoretical and numerical combustion," 2005.

[7] O. V. Vasilyev, "Solving multi-dimensional evolution problems with localized structures using second generation wavelets," *International Journal of Computational Fluid Dynamics*, vol. 17, no. 2, pp. 151–168, 2003.

[8] J. Regele and O. Vasilyev, "An adaptive wavelet-collocation method for shock computations," *International Journal of Computational Fluid Dynamics*, vol. 23, no. 7, pp. 503–518, 2009.